iScience

CellPress
OPEN ACCESS

Article

The Prc and CtpA proteases modulate cell-surface signaling activity and virulence in *Pseudomonas aeruginosa*

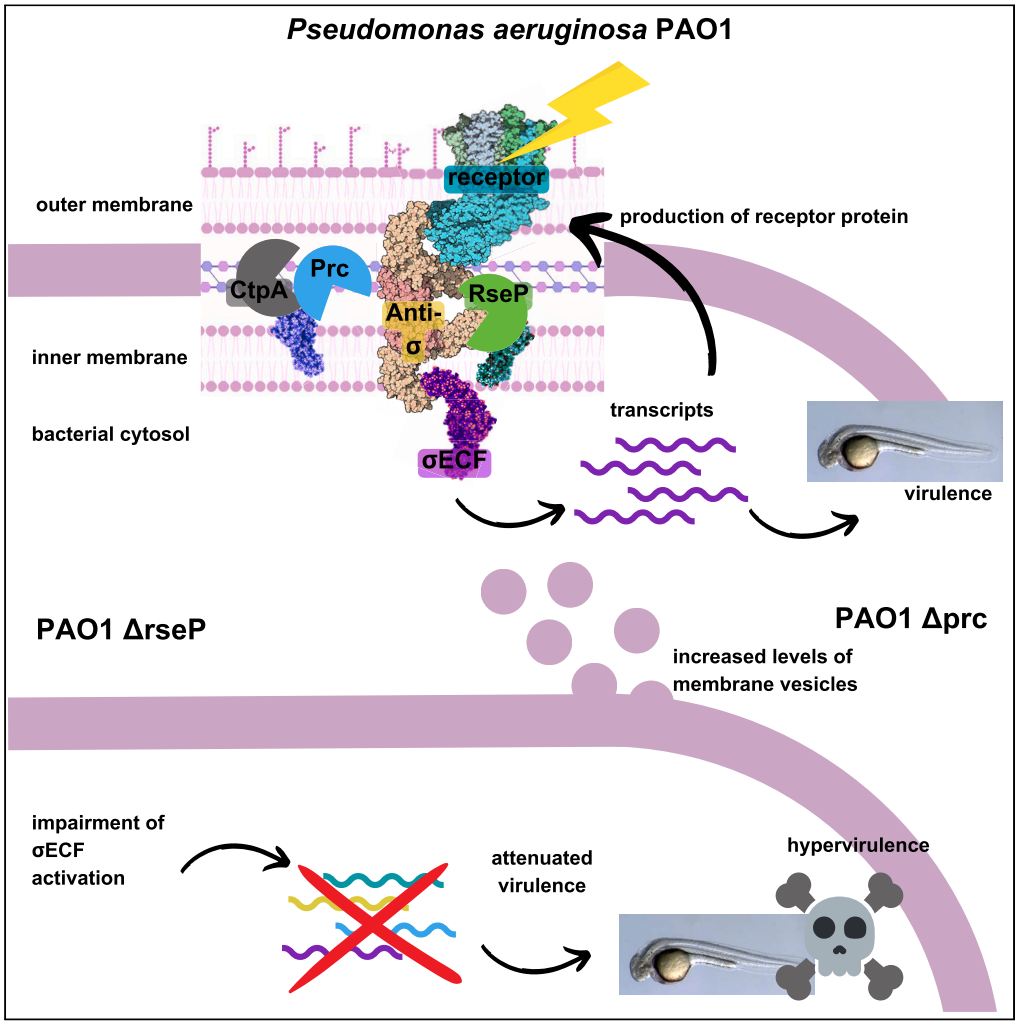

Joaquín R. Otero-Asman, Ana Sánchez-Jiménez, Karlijn C. Bastiaansen, ..., Alicia García-Puente, Wilbert Bitter, María A. Llamas

marian.llamas@eez.csic.es

Highlights

The Prc, CtpA, and RseP proteases modulates σ^{ECF} factors activity in *Pseudomonas*

A *P. aeruginosa rseP* mutant is attenuated in virulence and less cytotoxic

Mutation of *ctpA* gene decreases the virulence of *P. aeruginosa*

Lack of Prc increases membrane vesicles production and virulence of *P. aeruginosa*

Otero-Asman et al., iScience *26*, 107216
July 21, 2023
https://doi.org/10.1016/j.isci.2023.107216

iScience

CellPress
OPEN ACCESS

Article

The Prc and CtpA proteases modulate cell-surface signaling activity and virulence in *Pseudomonas aeruginosa*

Joaquín R. Otero-Asman,[1] Ana Sánchez-Jiménez,[1] Karlijn C. Bastiaansen,[1,2] Sarah Wettstadt,[1] Cristina Civantos,[1] Alicia García-Puente,[1] Wilbert Bitter,[2] and María A. Llamas[1,3,*]

SUMMARY

Cell-surface signaling (CSS) is a signal transfer system of Gram-negative bacteria that produces the activation of an extracytoplasmic function σ factor (σ^{ECF}) in the cytosol in response to an extracellular signal. Activation requires the regulated and sequential proteolysis of the σ^{ECF}-associated anti-σ factor, and the function of the Prc and RseP proteases. In this work, we have identified another protease that modulates CSS activity, namely the periplasmic carboxyl-terminal processing protease CtpA. CtpA functions upstream of Prc in the proteolytic cascade and seems to prevent the Prc-mediated proteolysis of the CSS anti-σ factor. Importantly, using zebrafish embryos and the A549 lung epithelial cell line as hosts, we show that mutants in the *rseP* and *ctpA* proteases of the human pathogen *Pseudomonas aeruginosa* are considerably attenuated in virulence while the *prc* mutation increases virulence likely by enhancing the production of membrane vesicles.

INTRODUCTION

In the human pathogen *Pseudomonas aeruginosa*, extracytoplasmic function sigma (σ^{ECF}) factors control important biological functions required for bacterial survival and colonization of the host.[1] Activity of several *P. aeruginosa* σ^{ECF} factors is controlled through a signal transduction cascade known as cell-surface signaling (CSS) that together with an σ^{ECF} factor involves an outer membrane receptor and a membrane-embedded anti-σ factor[2] (Figure 1). The CSS receptor belongs to the TonB-dependent transporter (TBDT) family and is usually involved in both signal transduction and transport of the inducing signal. Transport occurs through the large β-barrel C-terminal domain of the protein and needs the energy provided by the TonB-ExbBD system[3] (Figure 1). Signaling occurs via a small N-terminal domain located in the periplasm of the bacteria that interacts with the CSS anti-σ factor[4] (Figure 1). CSS anti-σ factors typically are single-pass cytoplasmic membrane proteins that contain a large periplasmic C-domain and a short cytosolic N-domain known as anti-sigma domain (ASD). While the C-domain receives the signal from the receptor, the N-domain binds the σ^{ECF} factor and keeps it sequestered in absence of the inducing stimulus.[2] The signal-responsive protein of the CSS pathway is the σ^{ECF} factor, which on activation binds to the RNA polymerase (RNAP) and directs it to the promoter of the signal response genes initiating gene transcription.

CSS systems are extensively present in bacteria of the *Pseudomonas* genus, especially in *P. aeruginosa*, *P. putida* and *Pseudomonas protegens*, in contrast to for example *Escherichia coli* that contains only one.[1,2] Signaling systems increase the ability of bacteria to detect and survive in many different environments, a characteristic of *Pseudomonas*.[9,10] In this genus, CSS is mainly involved in the regulation of iron acquisition by sensing and responding to iron-chelating compounds like siderophores, iron-citrate or heme, but also in the regulation of bacterial competition and virulence.[1,2,11] Analyses of *Pseudomonas* CSS systems has revealed that CSS activation in response to the inducing signal requires the targeted proteolysis of the CSS anti-σ factor (Figure 1B). This occurs through regulated intramembrane proteolysis (RIP), a conserved mechanism in which a transmembrane protein is subjected to several proteolytic steps in order to liberate and activate a cytosolic effector.[12] The RIP of CSS anti-σ factors always involves the site-2 zinc metalloprotease RseP, which cuts within the transmembrane domain of the protein liberating the CSS σ^{ECF} factor into the cytosol (Figure 1B).[5–7,13] RseP substrate recognition and cleavage occurs through size-filtering rather than by the recognition of a specific sequence/motif.[14] In order to create a suitable substrate

[1]Department of Biotechnology and Environmental Protection, Estación Experimental del Zaidín-Consejo Superior de Investigaciones Científicas, 18008 Granada, Spain

[2]Department of Medical Microbiology and Infection Control, Amsterdam University medical centres, location VU University, 1081 HV Amsterdam, The Netherlands

[3]Lead contact

*Correspondence: marian.llamas@eez.csic.es

https://doi.org/10.1016/j.isci.2023.107216

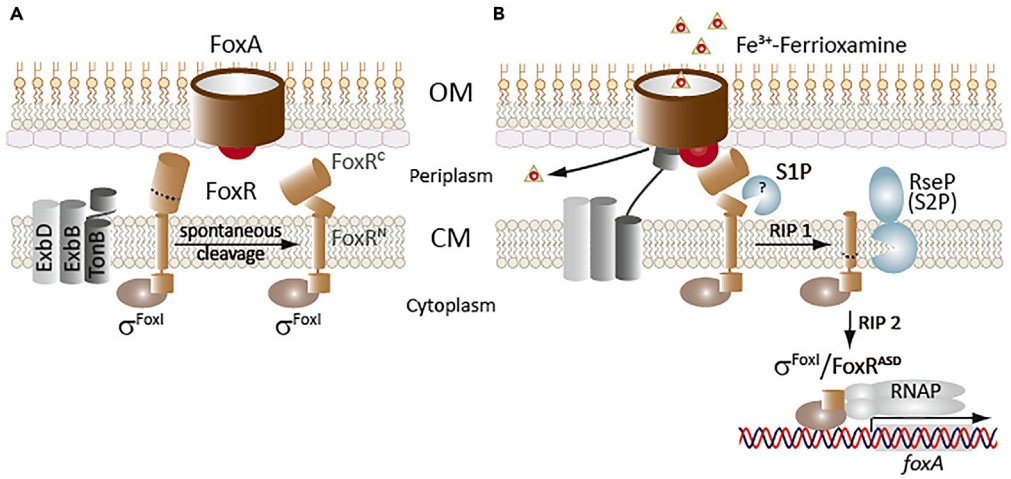

Figure 1. Model of the proteolytic cascade controlling CSS activation based on the *P. aeruginosa* Fox system

(A) The three components of the CSS system—receptor (FoxA), anti-σ factor (FoxR), and σ^{ECF} (σ^{FoxI})—and the TonB-ExbBD complex are shown. Prior to signal recognition, the *P. aeruginosa* FoxR anti-σ factor undergoes a spontaneous cleavage that produces two functional N- and C-domains that interact with each other in the periplasm and are both required for proper anti-σ factor function.

(B) Recognition of the siderophore ferrioxamine by the FoxA receptor produces the interaction of the TonB protein with FoxA enabling the energy coupled uptake of ferrioxamine. Binding of ferrioxamine to FoxA also promotes the interaction of the signaling domain of FoxA ($FoxA^{SD}$, red ball) with $FoxR^{C}$. This event triggers the regulated intramembrane proteolysis (RIP) of the $FoxR^{N}$ domain by the action of (at least) two proteases: a (still unidentified) site-1 protease (S1P) and the site-2 RseP protease (S2P). This results in the release of σ^{FoxI} into the cytoplasm bound to the anti-sigma domain of FoxR ($FoxR^{ASD}$). In several CSS pathways, including the *P. aeruginosa* Fox pathway, the ASD persists and is required for σ^{ECF} activity, having thus pro-σ activity. Although not experimentally demonstrated yet, this domain likely forms part of the transcription complex. Among other genes, σ^{FoxI} promotes the transcription of the *foxA* receptor gene. OM, outer membrane; CM, cytoplasmic membrane; RNAP, RNA polymerase. Adapted from[2] with the findings from.[5–8]

for RseP, the anti-σ factor needs to be cleaved by a site-1 protease on the periplasmic side. Evidence that a site-1 cleavage of CSS anti-σ factors occurs is the accumulation of a slightly larger fragment than the RseP product in *rseP* mutants.[6,7,11] However, the mechanism triggering this cleavage has not been identified yet. Our earlier analyses identified the carboxyl-terminal processing (CTP) serine protease Prc as the protease required for the site-1 cleavage of the IutY protein of *P. putida*.[6] IutY is a unique protein because it contains the σ^{ECF} and anti-σ factor domains fused in a single protein separated by a transmembrane domain. Prc is also required for activation of archetypal CSS systems,[6] but whether or not Prc directly cleaves these anti-σ factors has not been determined yet. This study aimed to shed light on these unknown features of CSS activation and resulted in the identification of a new protease, CtpA, involved in the activation of this signaling cascade.

RESULTS

The CTP serine protease *CtpA is involved in CSS activation*

Our previous results showed that absence of the Prc protease diminished but did not abolish *P. aeruginosa* CSS activity.[6] We hypothesized that this residual activity could be due to the function of another protease in the absence of Prc. *Pseudomonas* species produces a second carboxyl-terminal processing protease known as CtpA, a soluble periplasmic serine protease that in *P. aeruginosa* is involved in the activation of the σ^{SbrI} factor.[15,16] To test the effect of this protease in CSS activity, we introduced a *ctpA* deletion in *P. aeruginosa* (ΔctpA mutant) and assayed activity of the Fox and Fiu CSS systems, which respond to the siderophores ferrioxamine and ferrichrome, respectively. Activity of these systems was assayed using the CSS-dependent transcriptional fusions *foxA*:*lacZ* and *fiuA*:*lacZ*, containing the promoter region of the *foxA* or *fiuA* CSS receptor gene fused to a promoterless *lacZ* gene. Expression of these constructs completely depends on the activation of their respective CSS pathways.[6,17] As expected from previous results, lack of Prc reduced the activity of both CSS systems (Figure 2A). However, lack of CtpA did not reduce but considerably increased the response of the *P. aeruginosa* Fox and Fiu CSS systems to the presence of

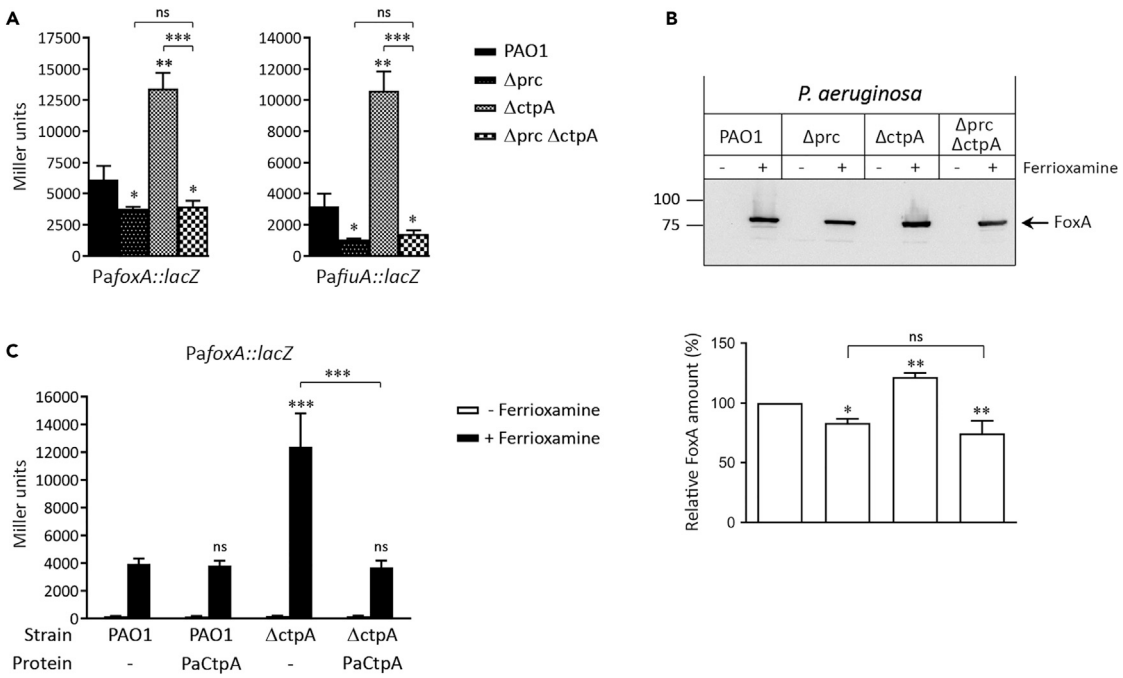

Figure 2. Activity of the *P. aeruginosa* Fox and Fiu CSS systems in *ctpA* mutants

(A and C) β-galactosidase activity of the indicated *P. aeruginosa lacZ* fusion gene in the PAO1 wild-type strain and the indicated isogenic mutant. Strains were grown under iron-restricted conditions with 1 μM ferrioxamine (Pa*foxA::lacZ*) or 40 μM ferrichrome (Pa*fiuA::lacZ*). In (C) strains bear the pBBR1MCS-5 empty (–) or the pBBR/PaCtpA plasmid (Table S1) next to the Pa*foxA::lacZ* fusion, and were grown in iron-restricted conditions without (–) or with (+) ferrioxamine. In (A and C) data are means ± SD from three biological replicates (N = 3). In (A) P-values were calculated by two-tailed *t*-test by comparing the value obtained in the mutant with that of the PAO1 wild-type strain in the same growth condition and in (C) by one-sample *t*-test. P-values are represented in the graphs by ns, not significant; *, $p < 0.05$; **, $p < 0.01$; ***, $p < 0.001$; and ****, $p < 0.0001$. Comparisons between other strains are indicated by brackets. (B) The indicated strains were grown in iron-restricted conditions without (–) or with (+) 1 μM ferrioxamine. Proteins were immunoblotted for FoxA using a polyclonal antibody. Position of FoxA and the molecular size marker (in kDa) is indicated. Blots are representative of three biological replicates (N = 3). The graph shows the intensity of the bands obtained with each strain normalized to the PAO1 strain and data are means ± SD from three biological replicates (N = 3). P-values were calculated by one-sample *t*-test to a hypothetical value of 100 by comparing the value obtained in the mutant with that of the PAO1 wild-type strain.

their cognate inducing siderophore (Figure 2A). Absence of this protease in *Pseudomonas putida* had a similar effect (Figure S1), showing a general role for CtpA in CSS activity. In accordance with increased *foxA* expression in the ΔctpA mutant and decreased in the Δprc mutant, production of the FoxA CSS receptor protein in response to ferrioxamine was higher in ΔctpA and lower in Δprc than in the wild-type PAO1 strain (Figure 2B). Activity of the Fox system in ΔctpA was not affected in the absence of the siderophore (Figure 2C), indicating that lack of CtpA does not lead to constitutive activation of the CSS pathways. Production of CtpA from a low-copy number plasmid did not affect the activity of the Fox system in the PAO1 wild-type strain but was able to complement the *P. aeruginosa* ΔctpA mutation (Figure 2C). This further indicates that CtpA modulates CSS activity. However, CtpA does not seem to compensate for the lack of Prc as initially hypothesized because the *ctpA* mutation resulted in increased instead of decreased CSS activity. Introduction of the *ctpA* deletion into the Δprc mutant did not alter the phenotype of the single Δprc mutant (Figures 2A and 2B). The lack of the ΔctpA phenotype in the Δprc ΔctpA double mutant suggests that CtpA works upstream of Prc in modulating CSS activity.

Absence of CtpA increases the amount of the FoxR anti-σ factor protein

We next focused on the identification of the CSS substrate of the *P. aeruginosa* Prc and CtpA proteases. We first considered the CSS anti-σ factor and analyzed the *P. aeruginosa* FoxR (PaFoxR) anti-σ factor. To detect PaFoxR, we used N- and C-terminally HA-tagged protein variants. PaFoxR is known to undergo a spontaneous cleavage that leads to a ~22 kDa N-domain ($FoxR^N$) and a ~16 kDa C-domain ($FoxR^C$) (Figure 1).[7,8] Both domains were detected by western blot in considerably higher amounts than the full-length protein (FoxR) (Figures 3A and 3B, PAO1 strain). In response to ferrioxamine, $FoxR^N$ is proteolytically processed by

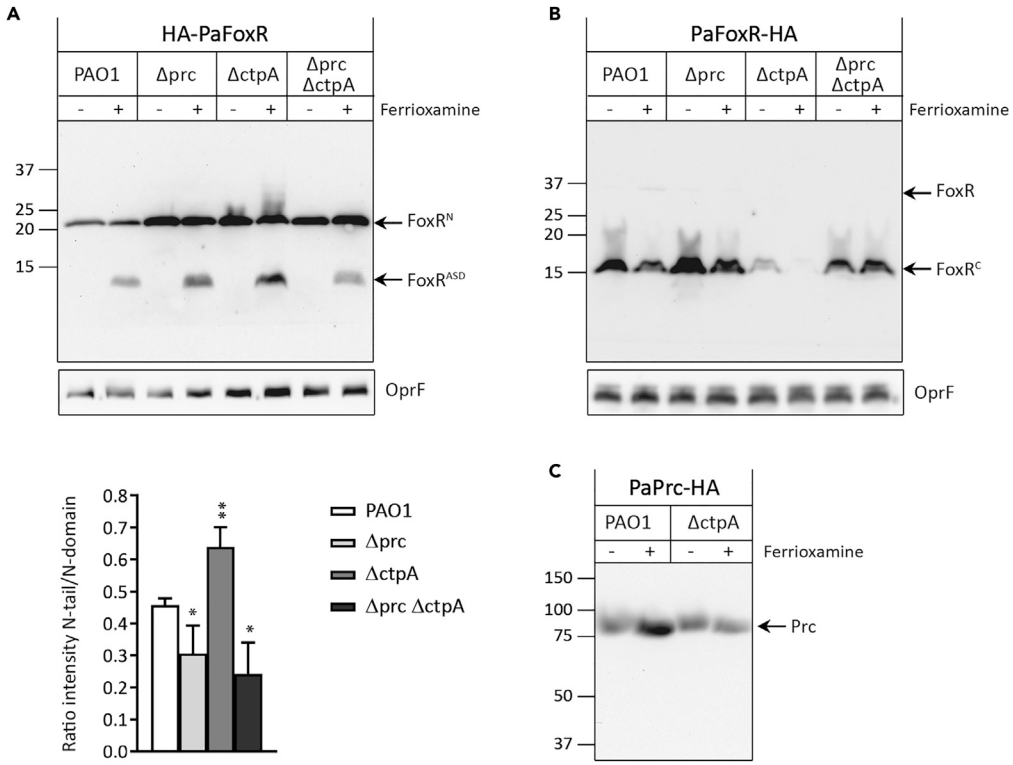

Figure 3. Role of the CtpA protease in processing *P. aeruginosa* CSS components

In all panels, the *P. aeruginosa* PAO1 wild-type strain and the indicated isogenic mutants were grown to late log-phase under iron-restricted conditions and in the absence (–) or presence (+) of 1 μM ferrioxamine. In (A) strains express an N-terminally HA-tagged *P. aeruginosa* FoxR protein (HA-PaFoxR), in (B) a C-terminally HA-tagged *P. aeruginosa* FoxR protein and in (C) a C-terminally HA-tagged Prc protein produced from pMMB67EH or pBBR1MCS-5 derived plasmids (see Table S1). Proteins were immunoblotted for HA using a monoclonal antibody. Position of the protein fragments and the molecular size marker (in kDa) is indicated. Presence of the HA-tag adds ~1 kDa to the molar mass of the protein fragments. Blots are representative of at least three biological replicates (N = 3). Detection of the OprF protein was used in (A) and (B) as loading control. The graph in (A) shows the ratio between the intensity of the $FoxR^{ASD}$ and the $FoxR^{N}$ domain bands, and data are means ± SD from three biological replicates (N = 3). P-values were calculated by two-tailed *t*-test by comparing the value obtained in the mutant with that of the PAO1 wild-type strain and are represented in the graphs by ns, not significant; *, $p < 0.05$; **, $p < 0.01$; ***, $p < 0.001$; and ****, $p < 0.0001$.

RIP through the action of an unknown site-1 protease and the RseP site-2 protease (Figure 1B).[7] RseP cuts within the transmembrane domain of $FoxR^{N}$ and generates $FoxR^{ASD}$ (Figure 1B), a domain that was detectable on ferrioxamine induction (Figure 3A). Lack of CtpA did not affect the RIP of $FoxR^{N}$ and the observed protein bands were obtained in the wild-type and ΔctpA strains (Figure 3A). However, the amount of the $FoxR^{N}$ domain, and especially that of the $FoxR^{ASD}$, was higher in the ΔctpA mutant (Figure 3A). Higher amounts of $FoxR^{ASD}$ usually correlates with increased CSS activity likely because this process produces the liberation and activation of the σ^{FoxI} factor,[6,7] a phenotype also observed in the ΔctpA mutant (Figure 2). Introduction of the Δprc mutation into the ΔctpA mutant reduced the amount of $FoxR^{ASD}$, which was similar to that obtained in the single Δprc mutant (Figure 3A). This is in agreement with the lower CSS activity observed in the Δprc ΔctpA double mutant (Figure 2). Of interest, the *ctpA* mutation had a considerable effect on the $FoxR^{C}$ domain, which was hardly detected in this mutant, especially in presence of ferrioxamine (Figure 3B). The amount of $FoxR^{C}$ in the Δprc ΔctpA double mutant was similar to that of the wild-type strain (Figure 3B), confirming that the *prc* mutation abolishes the effect of the *ctpA* mutation. Together, these results suggest that the PaFoxR anti-σ factor is not the substrate of CtpA although the absence of this protease considerably affects the stability of both domains of this protein.

Because the absence of CtpA lead to an increase of CSS activity in a Prc-dependent manner, we wondered whether Prc itself could be the substrate of CtpA. To analyze this, we used an HA-tagged Prc protein

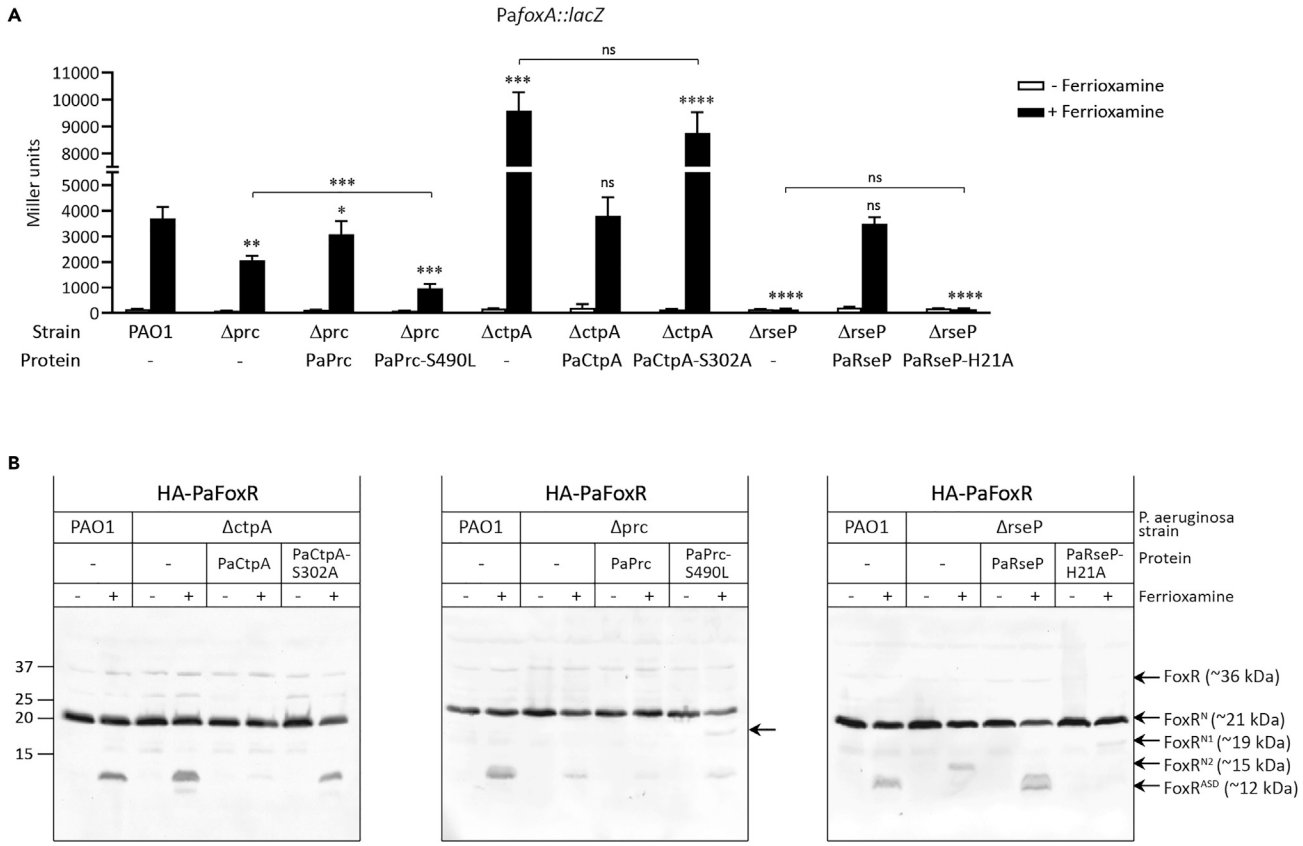

Figure 4. Effect of proteolytic inactive versions of the Prc, CtpA and RseP proteases on CSS activity and FoxR RIP

P. aeruginosa PAO1 wild-type strain and its isogenic Δprc, ΔctpA and ΔrseP mutants bearing a pBBR1MCS-5 derivative plasmid expressing the indicated *P. aeruginosa* protein and protein variant (-, empty plasmid) (Table S1) were grown under iron-restricted conditions without (–) or with (+) 1 μM ferrioxamine. In (A) strains also bear the *P. aeruginosa foxA::lacZ* fusion gene. β-galactosidase activity was determined as described in Materials and Methods and data are means ± SD from four biological replicates (N = 4). P-values were calculated by two-tailed *t*-test by comparing the value obtained in the mutant bearing the different protein variants with that obtained in the PAO1 wild-type strain in the same growth condition and are represented in the graphs by ns, not significant; *, $p < 0.05$; **, $p < 0.01$; ***, $p < 0.001$; and ****, $p < 0.0001$. Comparisons between other strains are indicated by brackets. In (B) strains express an N-terminally HA-tagged *P. aeruginosa* FoxR protein (HA-PaFoxR). Proteins were immunoblotted for HA using a monoclonal antibody. Position of the protein fragments and the molecular size marker (in kDa) is indicated. Presence of the HA-tag adds ~1 kDa to the molar mass of the protein fragments. Blots are representative of at least three biological replicates (N = 3).

expressed from a pBBR1MCS-5 derived plasmid (Table S1). The level of the Prc protease slightly increased in the wild-type strain in presence of ferrioxamine (Figure 3C, PAO1). This increase was not observed in the ΔctpA mutant (Figure 3C), which suggests that Prc is more stable when the Fox CSS system is active and that a CtpA-dependent function stabilizes Prc in this condition. Although Prc seems to be less stable in the absence of CtpA, this modest effect did not seem to affect CSS activity which was opposite in the ΔctpA single mutant with respect to the ΔctpA Δprc double mutant (Figure 2A).

The proteolytic activities of Prc, CtpA, and RseP are required for CSS activation

To further analyze the role of the *P. aeruginosa* Prc and CtpA proteases in the activation of CSS systems, we constructed proteolytically inactive versions of both proteases. Hereto, we changed the Prc active site protease residue Ser-490[18] to leucine and the CtpA active site residue Ser-302[19] to alanine. As control, the active site residue His-21 of the *P. aeruginosa* RseP protease[20] was changed to alanine. We then assayed the activity of the *P. aeruginosa* Fox CSS system in Δprc, ΔctpA and ΔrseP mutants complemented with either a wild-type Prc, CtpA or RseP protein or with the Prc-S490L, CtpA-S302A or RseP-H21A active site changed versions (Figure 4A). Activity of the Fox CSS pathway was considerably reduced in the Δprc mutant, highly increased in the ΔctpA mutant, and completely abolished in the ΔrseP mutant (Figure 4), as shown previously (Figure 2 and[6]). Complementation of the ΔctpA and ΔrseP mutants with the

corresponding wild-type protein restored CSS activity to PAO1 levels, while complementation of the Δprc mutant restored activity only partially (Figure 4A). The proteolytically inactivated versions of the proteases were unable to restore activity (Figure 4A). This confirms that the proteolytic activity of the three proteases is required for proper activity of the Fox CSS pathway. Of interest, the Prc-S490L active site mutant protein was not only unable to complement the Δprc mutation, but also exhibited a dominant negative effect by significantly decreasing the residual *foxA* promoter activity observed in the Δprc background in presence of ferrioxamine (Figure 4A). Similar results were obtained with active site changed versions of the Prc and RseP proteases of *P. putida* (Figure S2). While the wild-type versions of the *P. putida* Prc and RseP proteins were able to restore the ferrioxamine- and ferrichrome-induced CSS activity, the proteolytically inactive versions Prc-S485A and RseP-H23A were not (Figure S2). As observed in *P. aeruginosa*, the proteolytically inactivated version of Prc of *P. putida* significantly decreased the residual *foxA* and *fiuA* promoter activity obtained in the Δprc mutant (Figure S2), which confirms the dominant negative effect of this protein on CSS activity. Altogether, these results show the importance of the proteolytic action of Prc, CtpA and RseP proteases in activating CSS pathways.

Next, we assayed the effect of the proteolytically inactive versions of the three proteases on FoxR cleavage by Western-blot analyses. *P. aeruginosa* ΔctpA, Δprc and ΔrseP mutants producing an N-terminally HA-tagged FoxR protein and complemented with either the wild-type or the proteolytically inactive version of the protease were grown in absence and presence of ferrioxamine B (Figure 4B). The $FoxR^{N}$ domain (~21 kDa) was detected in similar amounts in all strains and conditions analyzed (Figure 4B). Ferrioxamine induction produced the $FoxR^{ASD}$ (~12 kDa) (Figure 4B, PAO1 strain) as a result of the RIP of the $FoxR^{N}$ domain.[7] As observed before (Figure 3A), this band was considerably more intense in the ΔctpA mutant, a phenotype that could be complemented with the wild-type CtpA protein but not with the inactive version CtpA-S302A (Figure 4B, left panel). These results are consistent with the Fox CSS activity observed in these strains (Figure 4A) relating higher amounts of $FoxR^{ASD}$ with increased CSS activity. Analysis of the FoxR cleavage in the Δprc mutant showed that the band corresponding to the $FoxR^{ASD}$ fragment was slightly less intense than in the PAO1 wild-type strain (Figure 4B, middle panel), as also observed before (Figure 3A). However, this phenotype could not be restored on complementation with the wild-type Prc protein and the amount of $FoxR^{ASD}$ fragment in this strain was also lower than in the PAO1 strain (Figure 4B, middle panel). In accordance, activity of the Fox CSS system was only partially restored in the complemented Δprc mutant (Figure 4A). Of interest, complementation with the proteolytically inactive version of Prc (PaPrc-S490L) resulted in the appearance of a new FoxR fragment of approximately ~19 kDa ($FoxR^{N1}$) (Figure 4B, middle panel). This band was also detected in the ΔrseP mutant complemented with the PaRseP-H21A variant but not with the wild-type RseP protein (Figure 4B, right panel). This protein fragment is larger than the FoxR product that accumulates in the ΔrseP mutant ($FoxR^{N2}$, ~15 kDa), which is the substrate of the RseP protease.[7] Presence of $FoxR^{N1}$ suggests that next the site-1 and site-2 cleavages (Figure 1) another proteolytic event takes place in response to ferrioxamine. Accumulation of $FoxR^{N1}$ only in the Δprc and ΔrseP mutants complemented with the proteolytically inactive version of the protease but not in the other strains suggests that Prc-S390L and RseP-H21A, by being inactive, impede the function of the protease that generates $FoxR^{N1}$ likely by interacting with this protease or its substrate.

Lack of RseP, Prc and CtpA proteases affects *P. aeruginosa* virulence

The CtpA protease has been shown to be required for *P. aeruginosa* virulence in a mouse model of acute infection,[16] but the role of RseP and Prc in virulence was not assayed yet. To analyze the pathogenicity of *P. aeruginosa* we used zebrafish (*Danio rerio*) embryos, which are lethally infected by this pathogen when the number of bacterial cells injected exceeds the phagocytic capacity of the embryo.[21–24] PAO1 wild-type strain and protease mutants were injected into the bloodstream of one-day-old embryos to generate a systemic infection and embryo survival was monitored during five days (Figure 5A). The ΔctpA mutant showed reduced virulence in zebrafish embryos compared to the wild-type strain ($p = 0.0004$) (Figure 5A), in accordance with the reduced virulence previously observed in mice.[16] The survival of the embryos injected with the ΔrseP mutant was similar to that of the control group injected only with phosphate-free physiological salt showing that this mutant was completely attenuated for virulence ($p < 0.0001$) (Figure 5A). In contrast, deletion of *prc* resulted in considerably more virulent strain than the PAO1 wild-type strain ($p = 0.0003$) (Figure 5A).

We also used the A549 human respiratory epithelial cell line as host since *P. aeruginosa* often colonizes the human respiratory tract. The cytotoxicity of *P. aeruginosa* toward the eukaryotic cells was determined by

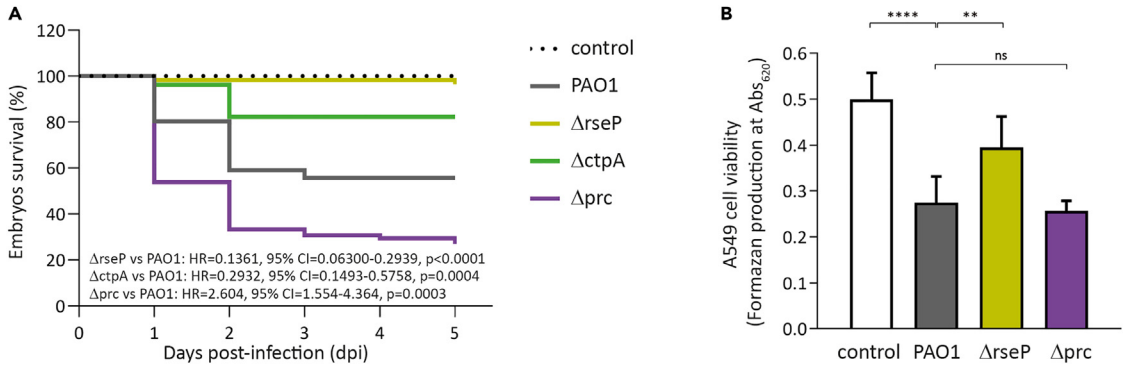

Figure 5. *P. aeruginosa* infections in zebrafish embryos and in the A549 cell line

(A) Kaplan-Meier zebrafish embryo survival curves on infection with *P. aeruginosa*. One-day-old embryos were injected with ~700–1000 CFU of the *P. aeruginosa* PAO1 wild-type strain or with the indicated isogenic mutant. Uninfected control (non-injected) is shown. Data are means ± SD of four biologically independent replicates (N = 4) with ~20 embryos/group in each replicate. The hazard ratio (HR), the 95% confidence interval ratio (95% CI), and the P-values (Log Rank Mantel-Cox) of each curve with respect to the reference PAO1 curve (HR = 1) are indicated.

(B) A549 cell viability. The *P. aeruginosa* PAO1 wild-type strain and the indicated isogenic mutant were co-incubated with the eukaryotic cells. Formazan production on addition of the MTT tetrazolium salt was determined spectrophotometrically at 620 nm. Uninfected cells (white bar) were used as control. Data are means ± SD from five biological replicates (N = 5). P-values were calculated by two-tailed *t*-test and are represented in the graphs by ns, not significant; *, $p < 0.05$; **, $p < 0.01$; ***, $p < 0.001$; and ****, $p < 0.0001$. Brackets indicate the comparison to which the P-value applies.

measuring A549 cell viability after co-incubation with the bacteria. The ΔrseP mutant was less efficient in damaging the A549 cells than the PAO1 wild-type strain, while the cytotoxicity of the Δprc mutant was similar to that of the wild-type strain (Figure 5B). In accordance, time-lapse imaging showed that the A549 cells detached after co-incubation with the wild-type strain but not with the ΔrseP mutant (Video S1). In fact, the percentage of detached cells was considerably lower following infection with the mutant ($p < 0.001$) (Figure S3). Detachment is the first indication of cell death. All together, these results indicate that lacks of RseP produces a considerably less virulent *P. aeruginosa* strain. In contrast, the cytotoxicity of the Δprc mutant was similar to that of the PAO1 wild-type strain (Figure 5B) suggesting that virulence traits other than cytotoxicity are responsible for the hypervirulent phenotype of this mutant.

Prc modulates the production of *P. aeruginosa* membrane vesicles (MVs)

An unexpected result from the virulence assays was the hyper-virulent phenotype of the Δprc mutant in zebrafish embryos (Figure 5). In *E. coli*, the Prc protease (also known as Tsp) modulates the activity of the murein DD-endopeptidase MepS, a hydrolase that cleaves peptidoglycan cross-links to insert new material.[25] The absence of Prc increases MepS levels and uncontrolled MepS activity increases the formation of membrane vesicles (MVs).[26] Because secretion of MVs is used by *P. aeruginosa* to deliver multiple virulence factors directly into the host cell cytoplasm,[27–29] we hypothesized that the hyper-virulent phenotype of the Δprc mutant could be related with increased MV production. SDS-PAGE and transmission electron microscopy (TEM) analyses showed that MVs production was indeed considerably higher in the Δprc mutant than in the PAO1 wild-type strain, a phenotype that could be complemented by providing the *prc* gene to the mutant in *trans* (Figures 6A and 6B). This indicates that the absence of Prc raises MV secretion, which would indeed increase *P. aeruginosa* virulence.

DISCUSSION

In recent years, it has become clear that regulated proteolysis is an important post-translational modification controlling the activity of several signal transduction pathways in bacteria.[30] Signal response proteins are often produced in an inactive state that prevents their interaction with the RNAP and/or the DNA in absence of the inducing signal. Because proteolysis is a fast and irreversible process, it allows for an immediate and longer response than other post-translational modification mechanisms. This may be beneficial in the control of processes like iron homeostasis, stress responses, development or virulence.[30] Moreover, regulated intramembrane proteolysis (RIP) has become increasingly recognized as one of the solutions to transmit extracytosolic signals to the cytosol through the cytoplasmic membrane.[12] By this mechanism, proteins are cleaved within the plane of the membrane liberating a cytosolic domain or protein able to modify gene transcription and thus elicit a response. The involvement of RIP in the control of

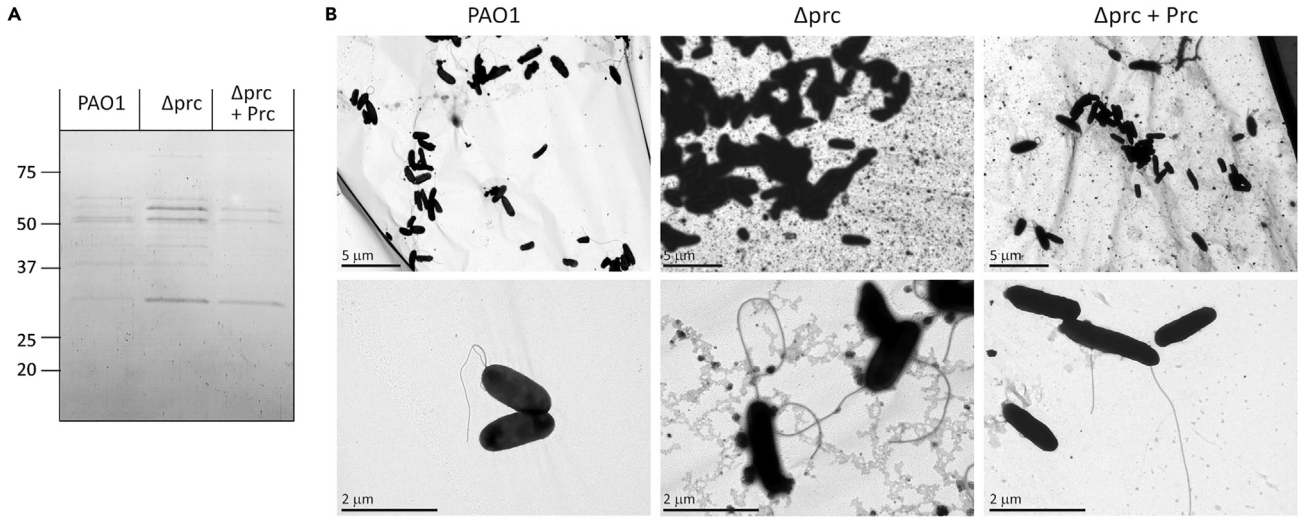

Figure 6. *P. aeruginosa* membrane vesicles (MVs) production and role of the Prc protease

P. aeruginosa PAO1 wild-type strain, the isogenic Δprc mutant, and the Δprc mutant bearing the pBBR/PAPrc plasmid (Table S1) (Δprc + Prc) were grown to exponential phase.

(A) Membrane vesicle (MV) proteins were isolated and visualized by Coomassie staining. Molecular size marker (in kDa) is indicated. SDS-PAGE is representative of three biological replicates (N = 3).

(B) Strains were negatively stained with phosphotungstic acid. TEM images were taken in several fields at 6.000 x and 25.000 x. Images are representative of three biological replicates (N = 3).

P. aeruginosa σ^{ECF} factors activity was first described for σ^{AlgU}, which promotes alginate production and the clinical relevant mucoid phenotype of *P. aeruginosa*.[31] Two proteases are required for σ^{AlgU} activation through RIP of is cognate membrane-embedded anti-σ factor MucA: the site-1 protease DegS (also known as AlgW) that also functions as the sensor protein of the signaling pathway and the site-2 protease RseP (also named MucP). In contrast to σ^{AlgU}/MucA, CSS σ^{ECF}/anti-σ factor pairs usually associate with an outer membrane receptor, which is the component of the signaling pathway that senses the inducing signal[1,2] (Figure 1). It is thus not surprising that DegS is not involved in activation of CSS σ^{ECF} factors.[6] RseP/MucP is also the site-2 protease of CSS anti-σ factors.[5–7,13] In accordance, inactivation of the proteolytic function of RseP completely blocks the activation of *Pseudomonas* CSS pathways (Figures 4A and S2). For RseP being able to cleave the CSS anti-σ factor, the anti-σ factor first needs to be cleaved by a site-1 protease that generates a smaller form of this protein suitable to enter the catalytic site of RseP.[6,7,11] The CTP serine protease Prc was the first identified protease involved in the site-1 cleavage of CSS anti-σ factors, specifically the hybrid σ^{ECF}/anti-σ factor protein IutY. In agreement, lack of Prc completely blocks activation of the Iut signaling pathway.[5,6] However, the activity of the Fox and Fiu CSS systems, in which the σ^{ECF} and anti-σ factor functions reside in two different proteins, is not completely null in a *prc* mutant (Figures 2 and[6,7]). Of interest, a proteolytically inactive version of Prc blocks the activity of CSS systems to a larger extend than the *prc* mutation in both *P. aeruginosa* and *P. putida* (Figures 4A and S2, Prc-S490L and Prc-S485A proteins, respectively). This confirms that the proteolytic activity of Prc is required to activate the CSS pathway. Moreover, the dominant negative effect exerted by the proteolytically inactive protein is likely the result of tight binding but not cleavage of the protease to its substrate, which avoids other proteolytic events to happen. Prc seems to be active under non-CSS inducing conditions,[5] which suggests that Prc function in absence of the signal is blocked by another element. This role could be performed by the CtpA protease, because lack of this protein increases CSS activation in a Prc-dependent manner (Figure 2). Both Prc and CtpA belong to the S41 family of CTP serine proteases,[32] which contain a PDZ domain located upstream the catalytic site required for substrate recognition and activity regulation.[18] *P. aeruginosa* Prc and CtpA are not orthologues; they have only 34% identity, differ in size (Prc is ~76 kDa and CtpA ~44 kDa) and belong to different CTP groups (Prc to the CTP-1 and CtpA to the CTP-3 group).[33] Western blot analyses of the *P. aeruginosa* FoxR anti-σ factor, which undergoes spontaneous cleavage immediately on production that separates the protein in a $FoxR^{N}$ and a $FoxR^{C}$ domain (Figure 1A), indicate that both Prc and CtpA modulate the levels of the $FoxR^{C}$ domain. Lack of CtpA reduces while that of Prc increases the stability of this domain (Figure 3B). This suggests that Prc

degrades $FoxR^C$ while CtpA prevents this degradation to occur. CtpA could perform this function by interacting directly with $FoxR^C$ protecting it from degradation or by inhibiting Prc function. We observed reduced instead of increased Prc protein level in the *ctpA* mutant (Figure 3C), which indicates that CtpA does not degrade Prc. Still, CtpA could act on another element required for Prc function. Interestingly, some CTP proteases partner with a lipoprotein that enhance the proteolysis process. For example, *P. aeruginosa* CtpA partners with the outer membrane lipoprotein LbcA[19,34] while the *E. coli* Prc protease associates with the NlpI lipoprotein.[35,36] Because several substrates of the *P. aeruginosa* CtpA protease are outer membrane lipoproteins,[19] CtpA could inhibit the function of Prc by degrading its partnering lipoprotein. The lipoprotein that associates with *P. aeruginosa* Prc has not been identified yet and further research is needed to test this hypothesis.

Deleting *ctpA* and *prc* does not prevent the RIP of the *P. aeruginosa* $FoxR^N$ domain on signal recognition (Figure 3A). Therefore, none of these proteases seems to be the site-1 protease that initiates the RIP pathway of the $FoxR^N$ domain in response to ferrioxamine (Figure 1B).[6,7] However, absence of CtpA increases the amount of the FoxR RIP product, the $FoxR^{ASD}$ (Figure 3A). This effect is likely due to the lack of the $FoxR^C$ domain in the *ctpA* mutant (Figure 3B) because it has been shown that $FoxR^C$ protects $FoxR^N$ from the RIP cascade.[7] In fact, when the $FoxR^C$ domain is absent, the activity of the Fox CSS pathway increases,[7] as also observed in the *ctpA* mutant (Figure 2A). Together, these results indicate that CtpA fine-tunes the activity of the *P. aeruginosa* Fox CSS pathway by preventing degradation and thus maintaining the correct levels of the $FoxR^C$ anti-σ factor domain, which in turn prevents the RIP of the $FoxR^N$ domain.

σ^{ECF}-mediated signaling controls important virulence functions in *P. aeruginosa*, including iron acquisition during infection, the response to the oxidative and cell envelope stress produced by components of the immune system of the host, synthesis of the exopolysaccharide alginate responsible of the virulent mucoid phenotype of *P. aeruginosa*, biofilm formation, and production of several virulence determinants (i.e. toxins, exoproteases, secretion systems and secreted proteins).[2,15,22,37,38] Therefore, we hypothesized that the proteases required for σ^{ECF} factor activation could be involved in *P. aeruginosa* virulence. Importantly, our results show that a mutant in the RseP protease, which is required for the activation of *P. aeruginosa* σ^{ECF} factors associated with transmembrane anti-σ factors,[1,2,11,38] is completely attenuated for virulence and shows significantly reduced cytotoxicity toward host cells (Figure 5 and Video S1). Although we cannot rule out the possibility that this effect may be due to the role of RseP in processing other transmembrane proteins, we believe that the inability of the *rseP* mutant to carry out σ^{ECF}-signaling also contributes to this phenotype. Furthermore, mutation of the CtpA protease reduced *P. aeruginosa* virulence in zebrafish embryos, as other authors observed in mice.[16] This phenotype is likely due to the impaired functioning of the type 3 secretion system (T3SS), which *P. aeruginosa* uses to inject toxic effectors into eukaryotic cells.[16] Surprisingly, mutation of the Prc protease produces a *P. aeruginosa* hyper-virulent strain in zebrafish embryos. In contrast, the *prc* mutation decreases the ability of a pathogenic *E. coli* strain to cause bacteremia and increases its sensitivity to complement-mediated serum killing.[39] The higher virulence of the *P. aeruginosa prc* mutant could be related to the increased production of MVs observed in this mutant (Figure 6). *P. aeruginosa* MVs are known to transport virulence factors to host cells and to promote inflammatory responses.[27,40,41] Further analyses will confirm this relation.

In summary, we report in this work the characterization of three proteases that directly or indirectly participate in the activation of *P. aeruginosa* σ^{ECF} factors, shedding more light on the complex proteolytic pathway that controls this process. Importantly, blocking signaling mechanisms required for crucial processes such as iron acquisition is an interesting strategy for drug development that would prevent pathogens from colonizing the host.[42] Proteases are druggable proteins and therefore proteases that modulate the activity of signaling systems required for pathogen's survival represent excellent drug targets. In fact, an inhibitor of the site-2 RseP protease was already shown to considerably decrease *E. coli* survival.[43] Identification and characterization of new regulatory proteases involved in bacterial signal transfer processes thus holds promise for the development of novel antibacterials.

Limitations of the study

We report in this study that the proteolytic activities of the periplasmic C-terminal processing proteases Prc and CtpA together with that of the cytoplasmic membrane-embedded site-2 zinc metalloprotease RseP are required for proper activation of CSS σ^{ECF} factors in *Pseudomonas*. Although we have established

that CtpA works upstream Prc in the proteolytic pathway that activates CSS systems, we have not yet identified the CSS substrate for this protease. Furthermore, we show that mutation in *rseP* and *ctpA* reduces *P. aeruginosa* virulence while mutation in *prc* increases bacterial virulence likely by enhancing the production of MVs. However, elucidation of the mechanistic details behind this observation requires further studies.

STAR★METHODS

Detailed methods are provided in the online version of this paper and include the following:

- KEY RESOURCES TABLE
- RESOURCE AVAILABILITY
  - Lead contact
  - Materials availability
  - Data and code availability
- EXPERIMENTAL MODEL AND STUDY PARTICIPANT DETAILS
  - Live vertebrates
  - Mammalian cell culture
  - Bacterial strains
- METHOD DETAILS
  - Bacterial growth conditions
  - Plasmid construction and molecular biology
  - Construction of mutant bacteria
  - β-galactosidase activity assay
  - SDS-PAGE and western-blot
  - Zebrafish maintenance, embryo care and infection procedure
  - Virulence assay in infected zebrafish embryos
  - Cytotoxicity assay in A549 human lung epithelial cells
  - Time-lapse imaging assay
  - Membrane vesicles (MVs) isolation and detection
  - Transmission electron microscopy (TEM)
- QUANTIFICATION AND STATISTICAL ANALYSIS

SUPPLEMENTAL INFORMATION

Supplemental information can be found online at https://doi.org/10.1016/j.isci.2023.107216.

ACKNOWLEDGMENTS

We thank A. Ocampo and F. Madrazo (Hospital Universitario Marqués de Valdecilla) for assistance with A549 cytotoxicity assays and time-lapse imaging, and K. K. Jim for assistance with the zebrafish embryo infections. This work was funded by MCIN/AEI/10.13039/501100011033 Spanish agency with projects BIO2017-83763-P and PID2020-115682GB-I00, and the PAIDI-2020 program of Junta de Andalucía (Spain) with project P18-FR-1621. JOA was supported by the Spanish Ministry of Economy through an FPI fellowship (BES-2013-066301).

AUTHOR CONTRIBUTIONS

J.O.A., W.B., and M.A.L. designed the study. J.O.A., K.B., A.S.J., S.W., C.C., and A.G.P. performed experiments. J.O.A., W.B., and M.A.L. contributed to the interpretation of the results. J.O.A. and M.A.L. wrote the manuscript with input from S.W. and W.B.

DECLARATION OF INTERESTS

The authors declare no competing interests.

INCLUSION AND DIVERSITY

We support inclusive, diverse, and equitable conduct of research.

Received: April 17, 2023
Revised: May 17, 2023
Accepted: June 22, 2023
Published: June 26, 2023

REFERENCES

1. Otero-Asman, J.R., Wettstadt, S., Bernal, P., and Llamas, M.A. (2019). Diversity of extracytoplasmic function sigma (σ^{ECF}) factor-dependent signaling in *Pseudomonas*. Mol. Microbiol. *112*, 356–373. https://doi.org/10.1111/mmi.14331.

2. Llamas, M.A., Imperi, F., Visca, P., and Lamont, I.L. (2014). Cell-surface signaling in *Pseudomonas*: stress responses, iron transport, and pathogenicity. FEMS Microbiol. Rev. *38*, 569–597. https://doi.org/10.1111/1574-6976.12078.

3. Noinaj, N., Guillier, M., Barnard, T.J., and Buchanan, S.K. (2010). TonB-dependent transporters: regulation, structure, and function. Annu. Rev. Microbiol. *64*, 43–60. https://doi.org/10.1146/annurev.micro.112408.134247.

4. Enz, S., Brand, H., Orellana, C., Mahren, S., and Braun, V. (2003). Sites of interaction between the FecA and FecR signal transduction proteins of ferric citrate transport in *Escherichia coli* K-12. J. Bacteriol. *185*, 3745–3752. https://doi.org/10.1128/JB.185.13.3745-3752.2003.

5. Bastiaansen, K.C., Civantos, C., Bitter, W., and Llamas, M.A. (2017). New insights into the regulation of cell-surface signaling activity acquired from a mutagenesis screen of the *Pseudomonas putida* IutY sigma/anti-sigma factor. Front. Microbiol. *8*, 747–815. https://doi.org/10.3389/fmicb.2017.00747.

6. Bastiaansen, K.C., Ibañez, A., Ramos, J.L., Bitter, W., and Llamas, M.A. (2014). The Prc and RseP proteases control bacterial cell-surface signalling activity. Environ. Microbiol. *16*, 2433–2443. https://doi.org/10.1111/1462-2920.12371.

7. Bastiaansen, K.C., Otero-Asman, J.R., Luirink, J., Bitter, W., and Llamas, M.A. (2015). Processing of cell-surface signalling anti-sigma factors prior to signal recognition is a conserved autoproteolytic mechanism that produces two functional domains. Environ. Microbiol. *17*, 3263–3277. https://doi.org/10.1111/1462-2920.12776.

8. Bastiaansen, K.C., van Ulsen, P., Wijtmans, M., Bitter, W., and Llamas, M.A. (2015). Self-cleavage of the *Pseudomonas* aeruginosa Cell-surface signaling anti-sigma factor FoxR occurs through an N-O acyl rearrangement. J. Biol. Chem. *290*, 12237–12246. https://doi.org/10.1074/jbc.M115.643098.

9. Spiers, A.J., Buckling, A., and Rainey, P.B. (2000). The causes of *Pseudomonas* diversity. Microbiology *146*, 2345–2350. https://doi.org/10.1099/00221287-146-10-2345.

10. Silby, M.W., Winstanley, C., Godfrey, S.A.C., Levy, S.B., and Jackson, R.W. (2011). *Pseudomonas* genomes: diverse and adaptable. FEMS Microbiol. Rev. *35*, 652–680. https://doi.org/10.1111/j.1574-6976.2011.00269.x.

11. Otero-Asman, J.R., García-García, A.I., Civantos, C., Quesada, J.M., and Llamas, M.A. (2019). *Pseudomonas aeruginosa* possesses three distinct systems for sensing and using the host molecule haem. Environ. Microbiol. *21*, 4629–4647. https://doi.org/10.1111/1462-2920.14773.

12. Brown, M.S., Ye, J., Rawson, R.B., and Goldstein, J.L. (2000). Regulated intramembrane proteolysis: a control mechanism conserved from bacteria to humans. Cell *100*, 391–398. https://doi.org/10.1016/s0092-8674(00)80675-3.

13. Draper, R.C., Martin, L.W., Beare, P.A., and Lamont, I.L. (2011). Differential proteolysis of sigma regulators controls cell-surface signalling in *Pseudomonas aeruginosa*. Mol. Microbiol. *82*, 1444–1453. https://doi.org/10.1111/j.1365-2958.2011.07901.x.

14. Hizukuri, Y., Oda, T., Tabata, S., Tamura-Kawakami, K., Oi, R., Sato, M., Takagi, J., Akiyama, Y., and Nogi, T. (2014). A structure-based model of substrate discrimination by a noncanonical PDZ tandem in the intramembrane-cleaving protease RseP. Structure *22*, 326–336. https://doi.org/10.1016/j.str.2013.12.003.

15. McGuffie, B.A., Vallet-Gely, I., and Dove, S.L. (2015). σ factor and anti-σ factor that control swarming motility and biofilm formation in *Pseudomonas aeruginosa*. J. Bacteriol. *198*, 755–765. https://doi.org/10.1128/JB.00784-15.

16. Seo, J., and Darwin, A.J. (2013). The *Pseudomonas aeruginosa* periplasmic protease CtpA can affect systems that impact its ability to mount both acute and chronic infections. Infect. Immun. *81*, 4561–4570. https://doi.org/10.1128/IAI.01035-13.

17. Llamas, M.A., Sparrius, M., Kloet, R., Jiménez, C.R., Vandenbroucke-Grauls, C., and Bitter, W. (2006). The heterologous siderophores ferrioxamine B and ferrichrome activate signaling pathways in *Pseudomonas aeruginosa*. J. Bacteriol. *188*, 1882–1891. https://doi.org/10.1128/JB.188.5.1882-1891.2006.

18. Chueh, C.K., Som, N., Ke, L.C., Ho, M.R., Reddy, M., and Chang, C.I. (2019). Structural basis for the differential regulatory roles of the PDZ domain in C-Terminal processing proteases. mBio *10*, e01129-19. https://doi.org/10.1128/mBio.01129-19.

19. Srivastava, D., Seo, J., Rimal, B., Kim, S.J., Zhen, S., and Darwin, A.J. (2018). A proteolytic complex targets multiple cell wall hydrolases in *Pseudomonas aeruginosa*. mBio *9*, e00972-18. https://doi.org/10.1128/mBio.00972-18.

20. Koide, K., Maegawa, S., Ito, K., and Akiyama, Y. (2007). Environment of the active site region of RseP, an *Escherichia coli* regulated intramembrane proteolysis protease, assessed by site-directed cysteine alkylation. J. Biol. Chem. *282*, 4553–4560. https://doi.org/10.1074/jbc.M607339200.

21. Clatworthy, A.E., Lee, J.S.W., Leibman, M., Kostun, Z., Davidson, A.J., and Hung, D.T. (2009). *Pseudomonas aeruginosa* infection of zebrafish involves both host and pathogen determinants. Infect. Immun. *77*, 1293–1303. https://doi.org/10.1128/IAI.01181-08.

22. Llamas, M.A., van der Sar, A., Chu, B.C.H., Sparrius, M., Vogel, H.J., and Bitter, W. (2009). A novel extracytoplasmic function (ECF) sigma factor regulates virulence in *Pseudomonas aeruginosa*. PLoS Pathog. *5*, e1000572. https://doi.org/10.1371/journal.ppat.1000572.

23. Llamas, M.A., and van der Sar, A.M. (2014). Assessing *Pseudomonas* virulence with nonmammalian host: zebrafish. Methods Mol. Biol. *1149*, 709–721. https://doi.org/10.1007/978-1-4939-0473-0_55.

24. Otero-Asman, J.R., Quesada, J.M., Jim, K.K., Ocampo-Sosa, A., Civantos, C., Bitter, W., and Llamas, M.A. (2020). The extracytoplasmic function sigma factor σ^{Vrel} is active during infection and contributes to phosphate starvation-induced virulence of *Pseudomonas aeruginosa*. Sci. Rep. *10*, 3139. https://doi.org/10.1038/s41598-020-60197-x.

25. Singh, S.K., Parveen, S., SaiSree, L., and Reddy, M. (2015). Regulated proteolysis of a cross-link-specific peptidoglycan hydrolase contributes to bacterial morphogenesis. Proc. Natl. Acad. Sci. USA *112*, 10956–10961. https://doi.org/10.1073/pnas.1507760112.

26. Schwechheimer, C., Rodriguez, D.L., and Kuehn, M.J. (2015). NlpI-mediated modulation of outer membrane vesicle production through peptidoglycan dynamics in *Escherichia coli*. Microbiologyopen *4*, 375–389. https://doi.org/10.1002/mbo3.244.

27. Bomberger, J.M., Maceachran, D.P., Coutermarsh, B.A., Ye, S., O'Toole, G.A., and Stanton, B.A. (2009). Long-distance delivery of bacterial virulence factors by *Pseudomonas aeruginosa* outer membrane vesicles. PLoS Pathog. *5*, e1000382. https://doi.org/10.1371/journal.ppat.1000382.

28. Koeppen, K., Hampton, T.H., Jarek, M., Scharfe, M., Gerber, S.A., Mielcarz, D.W., Demers, E.G., Dolben, E.L., Hammond, J.H., Hogan, D.A., and Stanton, B.A. (2016). A novel mechanism of host-pathogen interaction through sRNA in bacterial outer

membrane vesicles. PLoS Pathog. *12*, e1005672. https://doi.org/10.1371/journal.ppat.1005672.

29. Tashiro, Y., Uchiyama, H., and Nomura, N. (2012). Multifunctional membrane vesicles in *Pseudomonas aeruginosa*. Environ. Microbiol. *14*, 1349–1362. https://doi.org/10.1111/j.1462-2920.2011.02632.x.

30. Wettstadt, S., and Llamas, M.A. (2020). Role of regulated proteolysis in the communication of bacteria with the environment. Front. Mol. Biosci. *7*, 586497. https://doi.org/10.3389/fmolb.2020.586497.

31. Qiu, D., Eisinger, V.M., Rowen, D.W., and Yu, H.D. (2007). Regulated proteolysis controls mucoid conversion in *Pseudomonas aeruginosa*. Proc. Natl. Acad. Sci. USA *104*, 8107–8112. https://doi.org/10.1073/pnas.0702660104.

32. Rawlings, N.D., Waller, M., Barrett, A.J., and Bateman, A. (2014). MEROPS: the database of proteolytic enzymes, their substrates and inhibitors. Nucleic Acids Res. *42*, D503–D509. https://doi.org/10.1093/nar/gkt953.

33. Hoge, R., Laschinski, M., Jaeger, K.E., Wilhelm, S., and Rosenau, F. (2011). The subcellular localization of a C-terminal processing protease in *Pseudomonas aeruginosa*. FEMS Microbiol. Lett. *316*, 23–30. https://doi.org/10.1111/j.1574-6968.2010.02181.x.

34. Hsu, H.C., Wang, M., Kovach, A., Darwin, A.J., and Li, H. (2022). *Pseudomonas aeruginosa* C-Terminal processing protease CtpA assembles into a hexameric structure that requires activation by a spiral-shaped lipoprotein-binding partner. mBio *13*, e0368021. https://doi.org/10.1128/mbio.03680-21.

35. Kim, Y.J., Choi, B.J., Park, S.H., Lee, H.B., Son, J.E., Choi, U., Chi, W.J., and Lee, C.R. (2021). Distinct amino acid availability-dependent regulatory mechanisms of MepS and MepM levels in *Escherichia coli*. Front. Microbiol. *12*, 677739. https://doi.org/10.3389/fmicb.2021.677739.

36. Su, M.Y., Som, N., Wu, C.Y., Su, S.C., Kuo, Y.T., Ke, L.C., Ho, M.R., Tzeng, S.R., Teng, C.H., Mengin-Lecreulx, D., et al. (2017). Structural basis of adaptor-mediated protein degradation by the tail-specific PDZ-protease Prc. Nat. Commun. *8*, 1516. https://doi.org/10.1038/s41467-017-01697-9.

37. Hershberger, C.D., Ye, R.W., Parsek, M.R., Xie, Z.D., and Chakrabarty, A.M. (1995). The *algT (algU)* gene of *Pseudomonas aeruginosa*, a key regulator involved in alginate biosynthesis, encodes an alternative sigma factor (σ^E). Proc. Natl. Acad. Sci. USA *92*, 7941–7945. https://doi.org/10.1073/pnas.92.17.7941.

38. Chevalier, S., Bouffartigues, E., Bazire, A., Tahrioui, A., Duchesne, R., Tortuel, D., Maillot, O., Clamens, T., Orange, N., Feuilloley, M.G.J., et al. (2019). Extracytoplasmic function sigma factors in *Pseudomonas aeruginosa*. Biochim. Biophys. Acta. Gene Regul. Mech. *1862*, 706–721. https://doi.org/10.1016/j.bbagrm.2018.04.008.

39. Wang, C.Y., Wang, S.W., Huang, W.C., Kim, K.S., Chang, N.S., Wang, Y.H., Wu, M.H., and Teng, C.H. (2012). Prc contributes to *Escherichia coli* evasion of classical complement-mediated serum killing. Infect. Immun. *80*, 3399–3409. https://doi.org/10.1128/IAI.00321-12.

40. Ellis, T.N., and Kuehn, M.J. (2010). Virulence and immunomodulatory roles of bacterial outer membrane vesicles. Microbiol. Mol. Biol. Rev. *74*, 81–94. https://doi.org/10.1128/MMBR.00031-09.

41. Lee, J., Kim, O.Y., and Gho, Y.S. (2016). Proteomic profiling of Gram-negative bacterial outer membrane vesicles: Current perspectives. Proteomics. Clin. Appl. *10*, 897–909. https://doi.org/10.1002/prca.201600032.

42. Sánchez-Jiménez, A., Marcos-Torres, F.J., and Llamas, M.A. (2023). Mechanisms of iron homeostasis in *Pseudomonas aeruginosa* and emerging therapeutics directed to disrupt this vital process. Microb. Biotechnol. *16*, 1475–1491. https://doi.org/10.1111/1751-7915.14241.

43. Konovalova, A., Grabowicz, M., Balibar, C.J., Malinverni, J.C., Painter, R.E., Riley, D., Mann, P.A., Wang, H., Garlisi, C.G., Sherborne, B., et al. (2018). Inhibitor of intramembrane protease RseP blocks the σ^E response causing lethal accumulation of unfolded outer membrane proteins. Proc. Natl. Acad. Sci. USA *115*, E6614–E6621. https://doi.org/10.1073/pnas.1806107115.

44. Rawling, E.G., Martin, N.L., and Hancock, R.E. (1995). Epitope mapping of the *Pseudomonas aeruginosa* major outer membrane porin protein OprF. Infect. Immun. *63*, 38–42. https://doi.org/10.1128/iai.63.1.38-42.1995.

45. Jacobs, M.A., Alwood, A., Thaipisuttikul, I., Spencer, D., Haugen, E., Ernst, S., Will, O., Kaul, R., Raymond, C., Levy, R., et al. (2003). Comprehensive transposon mutant library of *Pseudomonas aeruginosa*. Proc. Natl. Acad. Sci. USA *100*, 14339–14344. https://doi.org/10.1073/pnas.2036282100.

46. Franklin, F.C., Bagdasarian, M., Bagdasarian, M.M., and Timmis, K.N. (1981). Molecular and functional analysis of the TOL plasmid pWWO from *Pseudomonas putida* and cloning of genes for the entire regulated aromatic ring meta cleavage pathway. Proc. Natl. Acad. Sci. USA *78*, 7458–7462. https://doi.org/10.1073/pnas.78.12.7458.

47. Sambrook, J., Fritsch, E.F., and Maniatis, T. (1989). Molecular Cloning: A Laboratory Manual (Cold Spring Harbor).

48. Choi, K.H., Kumar, A., and Schweizer, H.P. (2006). A 10-min method for preparation of highly electrocompetent *Pseudomonas aeruginosa* cells: application for DNA fragment transfer between chromosomes and plasmid transformation. J. Microbiol. Methods *64*, 391–397. https://doi.org/10.1016/j.mimet.2005.06.001.

49. Kaniga, K., Delor, I., and Cornelis, G.R. (1991). A wide-host-range suicide vector for improving reverse genetics in gram-negative bacteria: inactivation of the *blaA* gene of *Yersinia enterocolitica*. Gene *109*, 137–141. https://doi.org/10.1016/0378-1119(91)90599-7.

50. de Lorenzo, V., and Timmis, K.N. (1994). Analysis and construction of stable phenotypes in gram-negative bacteria with Tn5- and Tn10-derived minitransposons. Methods Enzymol. *235*, 386–405. https://doi.org/10.1016/0076-6879(94)35157-0.

51. Laemmli, U.K. (1970). Cleavage of structural proteins during the assembly of the head of bacteriophage T4. Nature *227*, 680–685. https://doi.org/10.1038/227680a0.

52. Renshaw, S.A., Loynes, C.A., Trushell, D.M.I., Elworthy, S., Ingham, P.W., and Whyte, M.K.B. (2006). A transgenic zebrafish model of neutrophilic inflammation. Blood *108*, 3976–3978. https://doi.org/10.1182/blood-2006-05-024075.

53. White, R.M., Sessa, A., Burke, C., Bowman, T., LeBlanc, J., Ceol, C., Bourque, C., Dovey, M., Goessling, W., Burns, C.E., and Zon, L.I. (2008). Transparent adult zebrafish as a tool for in vivo transplantation analysis. Cell Stem Cell *2*, 183–189. https://doi.org/10.1016/j.stem.2007.11.002.

54. Balsalobre, C., Silván, J.M., Berglund, S., Mizunoe, Y., Uhlin, B.E., and Wai, S.N. (2006). Release of the type I secreted alpha-haemolysin via outer membrane vesicles from *Escherichia coli*. Mol. Microbiol. *59*, 99–112. https://doi.org/10.1111/j.1365-2958.2005.04938.x.

55. Remuzgo-Martínez, S., Lázaro-Díez, M., Mayer, C., Aranzamendi-Zaldumbide, M., Padilla, D., Calvo, J., Marco, F., Martínez-Martínez, L., Icardo, J.M., Otero, A., and Ramos-Vivas, J. (2015). Biofilm formation and quorum-sensing-molecule production by clinical isolates of *Serratia liquefaciens*. Appl. Environ. Microbiol. *81*, 3306–3315. https://doi.org/10.1128/AEM.00088-15.

STAR★METHODS

KEY RESOURCES TABLE

REAGENT or RESOURCE	SOURCE	IDENTIFIER
Antibodies		
Mouse anti-HA.11 Epitope Tag Antibody	Biolegend	Cat. #901515; RRID: AB_2565334
Goat anti-Rabbit IgG (whole molecule)–Peroxidase	Sigma-Aldrich	Cat. #A0545; RRID: AB_257896
Rabbit anti-Mouse Immunoglobulins/HRP	Agilent DAKO	Cat. # P0260; RRID: AB_2636929
Rabbit anti-OprF (P. aeruginosa)	Gift from REW Hancock lab Rawling et al.[44]	N/A
Rabbit anti-FoxA (P. aeruginosa)	This paper	N/A
Bacterial and virus strains		
Bacterial strains	See Table S1 for a list of all bacterial strains	N/A
Chemicals, peptides, and recombinant proteins		
Deferoxamine mesylate salt	Merck Life Science	Cat. # D9533
Ferrichrome Iron-free	Santa Cruz Biotechnology. INC	Cat. #sc-255174
Phusion® Hot Start High-Fidelity DNA Polymerase	Thermo Fisher Scientific	Cat. #F630
Expand™ High Fidelity PCR System	Merck Life Science	Cat. #4738250001
o-Nitrophenyl-β-D-galactopyranoside (ONPG)	Merck Life Science	Cat. #369-07-3
Amersham™ Protran® Premium Western blotting membranes, nitrocellulose	Merck Life Science	Cat. #GE10600003
SuperSignal™ West Femto Maximum Sensitivity Substrate	Thermo Fisher Scientific	Cat. #34096
Ethyl 3-aminobenzoate methanesulfonate (Tricaine)	Merck Life Science	Cat. #E10521
Sea salts	Merck Life Science	Cat. #S9883
EZMTT Cell Proliferation Assay, MTT based	Merck Life Science	Cat. # CBA410
Deposited data		
Raw data for all figures (graphs, western-blot, microscopy pictures)	Mendeley Data repository	https://doi.org/10.17632/n4fwmnmy28.1
Experimental models: Cell lines		
A549 human lung epithelial cell	ATCC	Cat. #CCL-185
Experimental models: Organisms/strains		
Zebrafish roy^{a9}; mitfa^{w2}	ZIRC	Cat. #ZL1714
Oligonucleotides		
	See Table S2 for a list of all oligonucleotides	N/A
Recombinant DNA		
Plasmids	See Table S1 for a list of all plasmids	N/A
Software and algorithms		
GRAPHPAD PRISM version 9.5 for Windows	GraphPad by Dotmatics	N/A
ImageJ	National Institutes of Health (NIH)	N/A
Quantity One Analysis Software version 4.6.7	BioRad	N/A

RESOURCE AVAILABILITY

Lead contact

Further information and requests for resources and reagents should be directed to and will be fulfilled by the lead contact, María A. Llamas (marian.llamas@eez.csic.es).

Materials availability

All newly generated plasmids and bacterial strains associated with this paper are available by contacting the lead contact.

Data and code availability

- All data is available within the paper or supplemental information. Raw western blot images, and raw data used to generate graphs have been deposited at Mendeley and are publicly available as of the date of publication. The DOI is listed in the key resources table.
- This paper does not report original code.
- Any additional information required to reanalyse the data reported in this paper is available from the lead contact upon request.

EXPERIMENTAL MODEL AND STUDY PARTICIPANT DETAILS

Live vertebrates

Transparent adult casper mutant zebrafish (mitfa w2/w2;roy a9/a9) 44,45 were conserved at 26°C in aerated 5 L tanks with a 10/14 h dark/light cycle. Zebrafish embryos were collected during the first hour post-fertilization (hpf) and kept at 28°C in E3 medium supplemented with 0.3 mg/L methylene blue.

Mammalian cell culture

The A549 cell line (ATCC® CCL-185™) was maintained in DMEM medium supplemented with 10% (v/v) fetal bovine serum (FBS) (Gibco) in a 5% CO2 incubator at 37°C. Cells were tested for mycoplasma contamination, which was negative.

Bacterial strains

Strains used in this study are listed in Table S1. The wild-type *P. aeruginosa* PAO1 strain was obtained from the C. Manoil lab[45] and the *P. putida* KT2440 strain from the KN Timmis lab.[46] Bacteria were routinely grown in liquid LB[47] on a rotatory shaker at 37°C and 200 rpm.

METHOD DETAILS

Bacterial growth conditions

Bacteria were routinely grown in liquid LB[47] on a rotatory shaker at 37°C and 200 rpm. For low iron conditions, cells were cultured in CAS medium[17] containing 400 μM (for *P. aeruginosa*) or 200 μM (for *P. putida*) of 2,2′-bipyridyl. For induction experiments the low iron media was supplemented with 1 μM of iron-free ferrioxamine B (Merck Life Science) or 40 μM of iron-free ferrichrome (Santa Cruz Biotechnology). When required, 1 mM isopropyl β-D-1-thiogalactopyranoside (IPTG) was added to the medium to induce full expression from the pMMB67EH P*tac* promoter. Antibiotics were used at the following final concentrations (μg/mL): ampicillin (Ap), 100; gentamycin (Gm), 10; kanamycin (Km), 100; nalidixic acid (Nal), 25; piperacillin (Pip), 25; streptomycin (Sm), 100; tetracycline (Tc), 20.

Plasmid construction and molecular biology

Plasmids used are described in Table S1 and primers listed in Table S2. PCR amplifications were performed using Phusion® Hot Start High-Fidelity DNA Polymerase (Thermo Fisher Scientific) or Expand High Fidelity DNA polymerase (Merck Life Science). Chromosomal DNA from PAO1 or KT2440 was normally used as DNA template in PCR reactions except for the amplification of the *P. aeruginosa* proteolytically inactive versions of the proteases in which the pBBR1MCS-5 derivative plasmid bearing the wild-type version of the protease gene was used as template (pBBR/PaCtpA, pBBR/PaPrc and pBBR/PaRseP, respectively). All constructs were confirmed by DNA sequencing and transferred to *P. aeruginosa* or *P. putida* by electroporation.[48]

Construction of mutant bacteria

Construction of the ΔctpA mutants was performed by allelic exchange using a derived of the suicide vector pKNG101, the pKΔctpA plasmid (Table S1), which contains both a Sm resistance gene as a selectable marker for the cointegration event and the *Bacillus subtilis sacB* gene as a counter selectable marker to select for the allelic exchange.[49] The pKΔctpA plasmid was constructed by amplifying ~1 Kb DNA

fragments upstream and downstream of the respective deleted gene (the primers used are listed in Table S2). These fragments were ligated using an EcoRI site generated in the PCR reactions, and used as template in a second PCR reaction with the outer set of the primers of the first reactions. The final fragment, which contains XbaI-BamHI restriction sites, was cloned into the compatible restriction sites of pKNG101. The construct was sequenced to exclude the presence of point mutations in the sequences flanking the chromosomal deletion, and transferred to *P. aeruginosa* by triparental mating using the *E. coli* HB101 (pRK600) helper strain.[50] *P. aeruginosa* transconjugants bearing a cointegrate of the plasmid into the chromosome were selected on M9 minimal medium[47] with 0.3% (w/v) citrate as the sole carbon source and 100 μg/mL Sm. Sm-resistant transconjugants were analysed by PCR with primers flanking the *ctpA* gene. Those in which both the wild-type and the mutated gene product were amplified were selected and cultured in liquid LB medium without antibiotic during 5–6 h to promote the second crossover and the allelic exchange to occur. To select this process, colonies were plated on LB with 20% (w/v) sucrose. Sm-sensitive/sucrose-resistant colonies were analysed by PCR and southern-blot to confirm the chromosomal gene deletion.

β-galactosidase activity assay

β-galactosidase activities in soluble cell extracts were determined using *o*-nitrophenyl-b-D-galactopyranoside (ONPG) (Merck Life Science). Briefly, 1 mL of overnight cultures were centrifuged and the pellet resuspended in Z buffer (60 mM Na_2HPO_4, 40 mM NaH_2PO_4, 10 mM KCl, 1 mM $MgSO_4$, 2.7 mL β-mercaptoethanol, pH 7.0). Then, 0.1 mL of the cells were mixed with 0.5 mL Z buffer and cells were lysed by adding 20 μL SDS 0.05% (w/v) and 20 μL $CHCl_3$ followed by gentle vortexing for 1–2 min. Cell extracts were incubated 10 min at 30°C before adding 100 μL of a 4 mg/mL solution of ONPG in Z buffer. Reactions were stopped when the sample started to turn yellow by adding 260 mL of 1M Na_2CO_3. The incubation time i.e. time elapsed between the addition of ONPG and that of Na_2CO_3, was recorded. Reactions that did not turn yellow were stopped at 30–40 min after ONPG addition and the absorbance of all reactions was measured at 420 nm and 550 nm. The OD at 660 nm of the cultures was also measured. Miller units were calculated as follow: Miller units = $[(Abs_{420}-Abs_{550})*1000]/[OD_{660}$*incubation time (in min)*volume of cells (in mL)]. Each condition was tested in duplicate in at least three biologically independent experiments and the data given are the average of the three biologically independent experiments with error bars representing standard deviation (SD). Activity is expressed in Miller units.

SDS-PAGE and western-blot

P. aeruginosa was grown in iron-limited medium containing 1 mM IPTG (when necessary) and without or with 1 μM ferrioxamine. Cells were pelleted by centrifugation and heated for 10 min at 95°C following solubilisation in SDS-PAGE sample buffer.[51] Sample normalization was done according to the OD_{660} of the bacterial culture. Proteins were separated by SDS-PAGE containing 8, 12 or 15% (w/v) acrylamide and electrotransferred to nitrocellulose membranes (Merck Life Science). Ponceau S (Serva) staining was performed as a loading control. Immunodetection was realized using monoclonal antibody directed against the influenza hemagglutinin epitope (HA.11, Covance, Princeton, NJ) or polyclonal antibodies directed against the *P. aeruginosa* OprF[44] or FoxA proteins. The FoxA antibody was generated at Abyntek using the peptide SDTQFDHVKEERYAC as antigen. The second antibody, either the horseradish peroxidase-conjugated rabbit anti-mouse (Agilent DAKO) or the horseradish peroxidase-conjugated goat anti-rabbit IgG (Merck Life Science), was detected using the SuperSignal® West Femto Chemiluminescent Substrate (Thermo Fisher Scientific). Blots were scanned and analysed using the Quantity One version 4.6.7 (Bio-Rad). Images processing and band intensity measurements were performed using the ImageJ software.

Zebrafish maintenance, embryo care and infection procedure

Transparent adult casper mutant zebrafish (mitfa w2/w2;roy a9/a9)[52,53] were conserved at 26°C in aerated 5 L tanks with a 10/14 h dark/light cycle. Zebrafish embryos were collected during the first hour post-fertilization (hpf) and kept at 28°C in E3 medium (5.0 mM NaCl, 0.17 mM KCl, 0.33 mM $CaCl{\cdot}2H_2O$, 0.33 mM $MgCl_2{\cdot}7H_2O$) supplemented with 0.3 mg/L methylene blue. Prior to infection, 1day post-fertilization (dpf) embryos were mechanically dechorionated and anaesthetized in 0.02% (w/v) buffered 3-aminobenzoic acid methyl ester (pH 7.0) (Tricaine, Merck Life Science). Zebrafish embryos were individually infected by microinjection with 1 nl of P. aeruginosa in the caudal vein (systemic infection) as detailed described elsewhere.[23]

Virulence assay in infected zebrafish embryos

Zebrafish embryos were injected in the caudal vein with ~1000 CFU of exponentially grown *P. aeruginosa* cells previously suspended in phosphate-free physiological salt containing 0.5% (w/v) of phenol red. After infection, embryos were kept in 12-well plates containing 60 μg/mL of Sea salts (Merck Life Science) at 32°C with 20 individually injected embryos in each group per well. Embryo survival was determined by monitoring live and dead embryos at fixed time points during five days.

Cytotoxicity assay in A549 human lung epithelial cells

P. aeruginosa cytotoxicity on A549 cells was assayed using a colorimetric assay that detects the number of metabolically active eukaryotic cells able to cleave the MTT tetrazolium salt (Merck Life Science) to the insoluble formazan dye. The A549 cell line (ATCC® CCL-185™) was maintained in DMEM medium supplemented with 10% (v/v) fetal bovine serum (FBS) (Gibco) in a 5% CO_2 incubator at 37°C. One-day prior infection, the A549 cells were placed in 96-well plates at a concentration of 4 x 10^4 cells/well and cultured in phosphate-free DMEM medium (Gibco) with 5% (v/v) FBS. In this condition, cell mitosis does almost not occur. Late exponentially grown *P. aeruginosa* strains were then inoculated at a multiplicity of infection (MOI) of 20. At 3 hpi, 30 μl of a 5 mg/mL MTT solution in PBS was added to the wells and the plates were incubated for 2 h. The culture medium was then removed and 100 μl of dimethyl sulfoxide (DMSO) was added to solubilize the formazan. Production of formazan, which directly correlates to the number of viable cells, was quantified using a scanning multi-well spectrophotometer (Infinite® 200 PRO Tecan) at 620 nm.

Time-lapse imaging assay

Time-lapse microscopy was performed on a Nikon Eclipse Ti-E microscope (Nikon), equipped with a PlanFluor 20–40 × 0.6NA objective (Nikon) and a CO_2 incubator. A549 cells were seeded in coated 4-well μ-slides (Ibidi, Martinsried, Germany) in the same conditions as in the cytotoxic assays. Late exponentially grown *P. aeruginosa* strains were then inoculated at a multiplicity of infection (MOI) of 20. Images were collected from 0 to 240 min post-infection every 2 min with an ORCA- R2 CCD camera (Hamamatsu) powered by Nis Elements 3.2 software. Videos where edited with ImageJ.

Membrane vesicles (MVs) isolation and detection

P. aeruginosa MVs were isolated following the protocol described before[54] with some modifications. Briefly, overnight LB cultures of *P. aeruginosa* were diluted at 0.05 OD_{600}. At OD_{600} of ~1, the cultures were collected and centrifuged at 6.000 x g, 4°C. Approximately 10 mL of the supernatants were filtered through a 0.45 μm pore size filter (Millipore) to remove non-pelleted cells and the MVs were pelleted by ultracentrifugation at 150.000 x g, 180 min, 4°C. After carefully removal of the supernatant, the pellet was resuspended in PBS containing 15 % (v/v) glycerol in a volume proportional to the final OD_{600} of the culture and the amount of supernatant ultracentrifuged (e.g. 10 mL of supernatant of a 1.2 OD_{600} culture was resuspended in 120 μl of PBS-glycerol). 5 μl of the suspension was plated to verify that it was free of bacteria. MV proteins (40 μl) were separated by SDS-PAGE containing 15% (w/v) acrylamide and visualized by Coomassie staining.

Transmission electron microscopy (TEM)

TEM samples were prepared following the method described before.[55] Briefly, overnight cultures of *P. aeruginosa* were centrifuged at 0.6 x g and the pellets were washed four times in PBS. Bacteria cells were placed in 100 mesh copper grids containing the support carbon-coated Formvar film (Electron Microscopy Sciences) and air dried. Cells were negatively stained, with 1% (w/v) phosphotungstic acid in distilled water, for 20 secs and examined with a JEOL JEM-1011 transmission electron microscope equipped with an ORIUS SC 1000 CCD camera (GATAN).

QUANTIFICATION AND STATISTICAL ANALYSIS

Statistical analyses are based on *t*-test in which two conditions are compared independently. P-values from raw data (i.e. miller units from β-galactosidase assays) were calculated by independent two-tailed *t*-test, from ratio data to the control (i.e. FoxA production in Figure 2B) by one-sample *t*-test, and Kaplan-Meyer survival curves by Log-Rank (Mantel-Cox) using GRAPHPAD PRISM version 9.5 for Windows and are represented in the graphs by ns, not significant; *, $p < 0.05$; **, $p < 0.01$; ***, $p < 0.001$; and ****, $p < 0.0001$. Statistical details of the experiments can be found in the figure legends.